analytical chemistry

pubs.acs.org/ac Article

In Vivo Chemical Analysis of Plant Sap from the Xylem and Single Parenchymal Cells by Capillary Microsampling Electrospray Ionization Mass Spectrometry

Laith Z. Samarah, Tina H. Tran, Gary Stacey, and Akos Vertes*

Cite This: *Anal. Chem.* 2020, 92, 7299−7306 Read Online

ACCESS | Metrics & More | Article Recommendations | Supporting Information

ABSTRACT: In plants, long-distance transport of chemicals from source to sink takes place through the transfer of sap inside complex trafficking systems. Access to this information provides insight into the physiological responses that result from the interactions between the organism and its environment. In vivo analysis offers minimal perturbation to the physiology of the organism, thus providing information that represents the native physiological state more accurately. Here we describe capillary microsampling with electrospray ionization mass spectrometry (ESI-MS) for the in vivo analysis of xylem sap directly from plants. Initially, fast MS profiling was performed by ESI from the whole sap exuding from wounds of living plants in their native environment. This sap, however, originated from the xylem and phloem and included the cytosol of damaged cells. Combining capillary microsampling with ESI-MS enabled targeted sampling of the xylem sap and single parenchymal cells in the pith, thereby differentiating their chemical compositions. With this method we analyzed soybean plants infected by nitrogen-fixing bacteria and uninfected plants to investigate the effects of symbiosis on chemical transport through the sap. Infected plants exhibited higher abundances for certain nitrogen-containing metabolites in their sap, namely allantoin, allantoic acid, hydroxymethylglutamate, and methylene glutamate, compared to uninfected plants. Using capillary microsampling, we localized these compounds to the xylem, which indicated their transport from the roots to the upper parts of the plant. Differences between metabolite levels in sap from the infected and uninfected plants indicated that the transport of nitrogen-containing and other metabolites is regulated depending on the source of nitrogen supply.

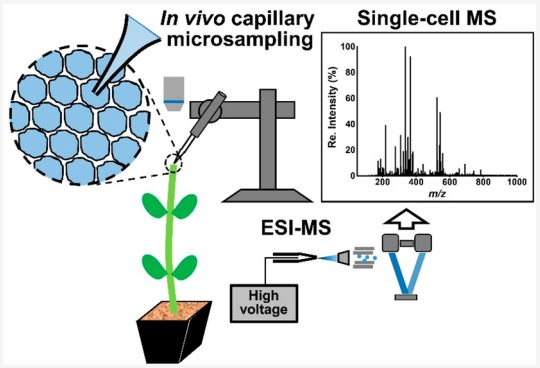

In vivo analysis enables the monitoring of biochemical responses to intrinsic and extrinsic stimuli by minimizing the effects of experimental factors that could alter the physiology of the organism.[1] Most in vivo studies by mass spectrometry have been focused on animal subjects, with relatively less attention given to plants.[2−4] In particular, the transport of metabolites in the sap through the plant vasculature would benefit from in vivo studies for understanding plant growth and survival.[5,6]

Of the crops that have been studied, there is particular interest in legumes, such as soybean (*Glycine max*), due to their ability to assimilate nitrogen through engaging in symbiosis with nitrogen-fixing bacteria.[7] In this interaction, nitrogen-fixing bacteria (e.g., *Bradyrhizobium japonicum*) infect the roots, resulting in the formation of specialized organs, called root nodules, where *B. japonicum* supplies nitrogen-containing raw material to the host that, in return, provides other nutrients to the bacteria. The nitrogenous assimilates are then transported in the sap to other parts of the plant through the vasculature.[8,9] Thus, in vivo sap analysis can provide information on plant physiology, especially in the context of its interaction with the environment.

Traditional methods employed for sap analysis usually involve taking the plant out of its original milieu and performing sample preparation that can alter the biochemical composition of the sap. For example, several studies used pressure chambers to collect sap from plants and measure the concentration for specific metabolites.[10,11] This approach involves cutting the plant stem or root and putting the fragment inside a pressurized chamber, where higher than ambient pressure is used to force the sap out of the cut surface.[10,11] Collected sap is then processed depending on the targeted molecules. As the conditions during sap collection differ significantly from the optimal conditions for plant

Received: March 2, 2020
Accepted: April 28, 2020
Published: April 28, 2020

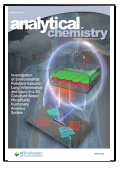

https://dx.doi.org/10.1021/acs.analchem.0c00939
Anal. Chem. 2020, 92, 7299−7306

growth, and because the collected sap is processed before analysis, the information that can be obtained under this method might not accurately reflect the physiology of the plant. In addition, these analytical approaches do not preserve spatial information that can be critical for understanding the biochemical processes behind the biosynthesis and transport of compounds.

In pursuit of achieving minimally invasive phenotypic and chemical analysis of plants, various imaging techniques have been applied, including hyperspectral imaging, fluorescence imaging, magnetic resonance imaging (MRI), and positron emission tomography (PET).[12] These methods can be characterized by their sensitivity, specificity, and molecular coverage. For example, positron emission tomography (PET) has been applied to study and image the transport of material in intact plants.[6,13−15] The advantages of this technique include the ability to obtain in vivo and real time dynamic information and map out locations with different metabolic activities. One inherent limitation, however, is its inability to chemically speciate the different labeled molecules. For example, by using $^{11}CO_2$, the spatial fate of ^{11}C-labeled photoassimilates was monitored throughout plants.[16] These measurements, however, did not provide information on the chemical transformations that took place downstream of $^{11}CO_2$ incorporation by the plant. In an effort to gain synergistic benefits from the combination of two imaging modalities, for example, MRI and PET have also been explored.[17]

Mass spectrometry (MS) is widely used for the analysis and imaging of a broad range of molecules in plants owing to its high sensitivity and specificity, its wide molecular coverage, and its ability to provide structural information.[18,19] Among the ionization methods used in MS, vacuum-based ionization sources, such as matrix-assisted laser desorption ionization (MALDI[20,21]) and matrix-free laser desorption ionization, e.g., from silicon nanopost arrays,[22] require the sample to be placed under high vacuum, a condition that interferes with the viability of the organism. However, newly emerging ambient ionization platforms can be operated under conditions that are suitable for in vivo analysis. Some of the ambient ionization methods that have been successfully employed for in vivo analysis include desorption electrospray ionization (DESI),[23] laser ablation electrospray ionization (LAESI),[24,25] direct analysis in real time (DART),[26] leaf spray,[27] and related techniques.[28,29]

Although minimizing perturbation of the organism is an essential part of in vivo analysis, the plant may still be subjected to some degree of sample preparation. For example, some parts, such as the leaf epidermis, are more easily accessible for ambient MS analysis than other parts, e.g., sap, that require certain invasive procedures for analysis. For example, in leaf-spray MS, a small incision is made on the leaf to facilitate spray formation from the plant sap.[27] Despite the applied invasive action necessary for making certain parts of the organism accessible to the analytical technique, the analysis can still be classified as in vivo as long as the organism remains viable and the induced perturbation has minimal effect on the measured properties.

In vascular plants, transport of materials takes place in different parts of the vasculature, e.g., xylem and phloem, depending on the flow direction of the compounds in demand. Additionally, cells that neighbor these conduits in the vasculature have different biological functions. Probing the chemical compositions of these different cell types in vivo requires sensitive and selective (high spatial resolution) ambient analytical sampling methods, e.g., single-cell MS techniques. Current ambient single-cell MS techniques include fiber-based LAESI (f-LAESI),[30,31] atmospheric pressure MALDI (AP-MALDI),[32] nanospray-DESI,[33] capillary microsampling ESI-MS,[34,35] and other related techniques.[36,37] Capillary microsampling ESI-MS is a probe sampling technique that utilizes a capillary with a tapered tip and a micromanipulator to extract cellular content. The capillary containing cellular extract is then used as a nanospray emitter to generate ions. Reported capillary tip diameters that were used for single-cell MS were ∼1 μm,[35] in comparison with reported fiber tip diameters of ∼15 μm in f-LAESI,[30] and spatial resolution of ∼1 μm in single-cell AP-MALDI.[32]

Here we describe two methods for in vivo analysis of sap from plants, direct and capillary microsampling[38] electrospray ionization mass spectrometry (ESI-MS). The first method enabled fast analysis of whole sap (i.e., sap from the xylem, phloem, and other cells in the pith) exudate spontaneously formed by natural upward flow of sap through the plant vasculature after cutting the stem. Plants analyzed by this method remained in their pots during the analysis to minimize external perturbations to their native environment and remained viable after the analysis. Capillary microsampling provided higher selectivity for sampling sap native to specific parts of the plant stem. Using these two methods, certain physiological responses in *G. max* to infection by the microsymbiont, *B. japonicum*, were investigated. Specifically, we observed that sap from infected *G. max* exhibited higher abundances for certain nitrogen-containing metabolites, namely allantoin, allantoic acid, hydroxymethylglutamate, and methylene glutamate, compared to uninfected plants. Using capillary microsampling, we localized these compounds to the xylem, which indicated their transport from the roots to the upper parts of the plant. Collectively, these differences in metabolite levels between sap of infected and uninfected plants indicated that the transport of nitrogen and other metabolites is regulated depending on the nitrogen source. The metabolite compositions for other parts of the plant's vasculature, i.e., parenchymal cells in the pith, were also profiled using capillary microsampling.

EXPERIMENTAL SECTION

***B. japonicum* Cultures.** Culturing of wild-type *B. japonicum* strain USDA110 was described in previous publications.[39,40] Briefly, cultures of *B. japonicum* USDA110 were incubated, with shaking, for 3 days at 30 °C in HM salts medium containing 25 mg/L of tetracycline and 100 mg/L of spectinomycin.[41] To estimate the bacterial cell counts in the cultures, the optical density at a wavelength of 600 nm was measured (DeNovix DS-C, DeNovix Inc., Wilmington, DE). When the optical density reached 0.8 (or 10^8 cells/mL), the culture tubes were removed from the incubator, centrifuged at 3000 rpm for 10 min, and washed three times with sterile deionized water. Finally, sterile deionized water was added to the rhizobia pellet and vortexed to form a homogeneous solution that was used later for inoculating soybean seeds.

***G. max* Growth and Inoculation with *B. japonicum*.** *G. max* seeds of "Williams 82" were surface sterilized with 20% (v/v) bleach for 10 min and rinsed five times with sterile water. The sterile seeds were planted into pots containing a mixture of sterilized 3:1 vermiculite:perlite. For inoculation, 500 μL of the solution containing *B. japonicum* were added to each

https://dx.doi.org/10.1021/acs.analchem.0c00939
Anal. Chem. 2020, 92, 7299−7306

sterilized soybean seed. After covering the seeds with potting material, the pots were placed in a growth chamber (Percival E36HO, Percival Scientific, Perry, IA) at 30 °C with a 16-h light/8-h dark cycle. The plants were supplied with B & D medium,[42] a solution containing essential minerals for legumes inoculated with nitrogen-fixing bacteria. Uninfected plants were grown similarly without inoculation with *B. japonicum* and were supplied with B & D medium containing 5 mM of KNO_3. After 21 days of growth, the plants were taken out of the chamber and analyzed within 1 min (Figure S1).

Direct ESI-MS. Thin-wall glass capillaries (TW100F-3, World Precision Instruments, Sarasota, FL) were pulled using a micropipette puller (P-1000, Sutter Instrument, Novato, CA) with a box filament (FB255B, Sutter Instrument, Novato, CA). The following pulling settings were used: heat = 486, pull = 10, velocity = 30, delay = 250, and pressure = 500. Capillaries with ∼3 μm tip diameter were produced. The pulled capillary was backfilled with 5 μL of electrospray solution (1:1:1 acetonitrile:methanol:water with 0.1% acetic acid (v/v), and 2:1 methanol:chloroform for analysis in positive and negative ion mode, respectively) and mounted on a quick-release cylindrical device mount (HFF001, Thorlabs Inc., Newton, NJ).

A microloader pipet tip (cat. no. 930001007, Eppendorf, Hauppauge, NY) was cut to ∼2.5 cm in length and was inserted into the pulled glass capillary with one of its ends protruding out of the blunt side of the capillary (Figure 1). A

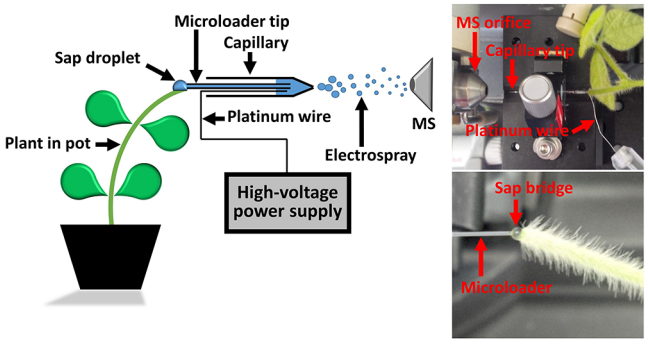

Figure 1. Schematic representation and photographic images of the experimental setup for direct ESI-MS of sap exudate produced spontaneously by cutting a plant stem. A microloader is inserted into a pulled capillary backfilled with electrospray solution. Sap flows through the microloader tip by capillary action and mixes with the electrospray solution, and the mixture is ionized by applying high voltage to a platinum wire that is in contact with the mixture.

platinum wire (Alfa Aesar, Ward Hill, MA) of 100 μm in diameter and ∼5 cm in length, held by a microelectrode holder (MEW-F10A, Warner Instruments, Hamden, CT, USA), was inserted into the capillary from the back until it came in contact with the solution. Alternatively, a pulled glass capillary (tip diameter ∼1 μm) coated with a conductive material (Glasskit-10-CE, New Objective, Woburn, MA) was used, and the platinum wire was fixed in position to make contact with the outer conductive surface of the capillary. Either way, the capillary tip was positioned at ∼5−10 mm away from the orifice of a quadrupole time-of-flight (TOF) mass spectrometer equipped with a traveling wave ion mobility separation (IMS) system (Synapt G2-S, Waters Co., Milford, MA).

A plant was taken out of the growth chamber and kept in its pot. The plant stem was cut with a sterile scalpel ∼5 mm below the shoot apical meristem, resulting in the formation of a sap droplet (volume ∼1 μL) (Figure S1d and Figure 1). The freshly cut surface of the plant stem was positioned to form a sap bridge with the rear end of the microloader tip, causing sap to flow through the microloader tip and mix with the electrospray solution by capillary action. To generate an electrospray, high voltage (3.4 kV and −2.4 kV for positive and negative ion mode, respectively) was applied to the microelectrode by a power supply (PS350, Stanford Research Systems, Inc., Sunnyvale, CA). A schematic representation and photographic images of the experimental setup for direct ESI-MS are shown in Figure 1.

After the analysis was completed, the plant was placed back in the growth chamber and visual signs of growth, such as lateral shoot development and plant height, were monitored daily, up to 14 days postanalysis.

Capillary Microsampling ESI-MS. The experimental procedures for capillary microsampling ESI-MS were detailed in a previous publication.[43] Briefly, a thin-wall glass capillary pulled as described above and backfilled with electrospray solution (same composition as mentioned above) was held by a capillary holder (IM-H1, Narishige, Tokyo, Japan) that was mounted on a motorized micromanipulator (TransferMan NK2, Eppendorf, Hauppauge, NY). To visualize the sampling of sap from selected parts of the vasculature, the micromanipulator was mounted on an upright microscope (BX43, Olympus, Tokyo, Japan). A ∼2 cm long segment was excised from the plant stem ∼5 mm below the apical meristem and held on a glass microscope slide using double-sided adhesive tape. The capillary holder with the pulled capillary was mounted on the micromanipulator at 60° relative to the surface of the cut stem. During transverse cutting of the plant shoot, it is possible that sap from different parts of the stem can mix and cover the cut surface, which could skew the composition obtained by local sap sampling when the capillary tip makes contact with the surface. Thus, to minimize sampling of whole sap, the cut surface was left to air-dry for ∼1 min. A schematic representation of the capillary microsampling setup is shown in Figure 2. During sampling, the capillary was carefully lowered until it was immersed into the selected part of the stem. To withdraw sap, negative pressure was applied using a syringe that was connected to the capillary holder, which resulted in sampling ∼1 pL of sap. The capillary was then removed from the holder and placed on a quick release cylindrical device mount (HFF001, Thorlabs Inc., Newton, NJ) to position the capillary tip ∼5 mm away from the MS orifice. A high voltage was applied to the solution through a platinum wire inserted from the back as described above.

Comparative Multivariate Statistical Analysis. Raw mass spectra acquired from sap of infected and uninfected plants were processed using the mMass software (http://www.mmass.org/) for deisotoping, peak picking (for peaks with S/N ≥ 3), and subtraction of background spectra from the electrospray solution. The resulting peak lists and ion intensities were imported into MetaboAnalyst 4.0 (https://www.metaboanalyst.ca/), wherein the peak intensities were normalized by sum, and Pareto scaling was performed, followed by comparative multivariate statistical analysis that was represented by PCA scores plot, volcano plot, and box-and-whisker plots. Statistical significance represented by *p*-values was determined using the *t*-test.

https://dx.doi.org/10.1021/acs.analchem.0c00939
Anal. Chem. 2020, 92, 7299−7306

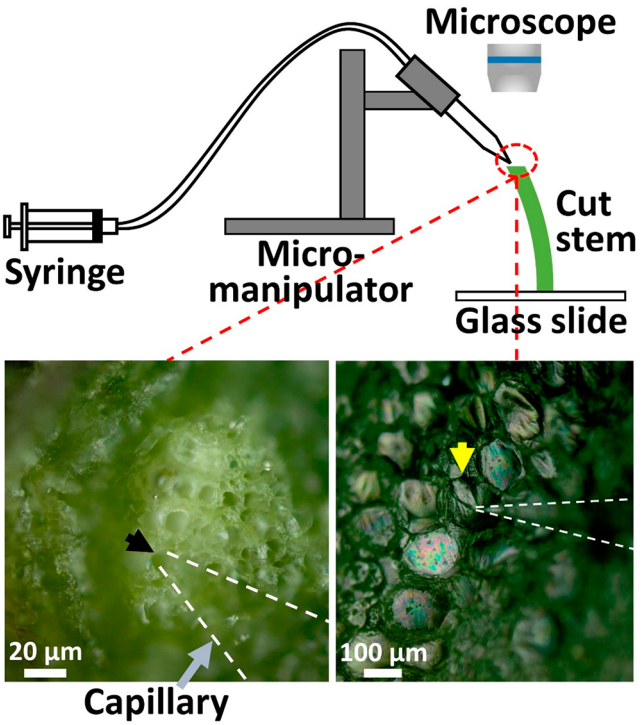

Figure 2. Capillary microsampling of xylem sap and single parenchymal cells in the pith. A stem segment is cut from a plant and held on a glass slide by double-sided adhesive tape, and the cut surface is visualized under an upright microscope. A pulled capillary held by the micromanipulator is inserted into the xylem (black arrow) or into a parenchymal cell from the pith (yellow arrow), and the sap is drawn into the capillary by a syringe.

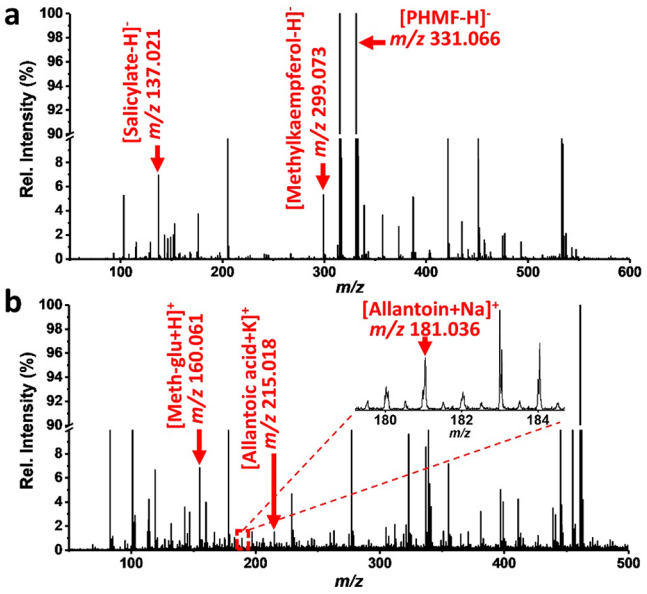

Figure 3. Representative (a) negative and (b) positive ion mode mass spectra produced from whole sap by direct ESI-MS. Soybean plants were studied 21 days postinoculation with *B. japonicum*. PHMF: pentahydroxymethoxyflavanone.

RESULTS AND DISCUSSION

Direct ESI-MS of Whole Sap from Living Plants. Mass spectra produced by direct ESI-MS of whole sap exuded from soybean plants contained peaks that corresponded to diverse types of endogenous compounds. Sugars, amino acids, flavonoids, glycosides, vitamins, plant hormones, and lipids were all detected by direct ESI-MS (Figure 3 and Table S1). These chemical species may originate from different parts of the stem, as whole sap is a mixture of compounds from the xylem, phloem, and cells in other parts, such as the pith.

The ion signal duration from a sap droplet typically lasted between ~2 to 4 min (Figure S2a). This enabled the selection of several ions of interest per sample for fragmentation by collision-induced dissociation (CID). The ion signal intensity diminished as the electrospray solution inside the capillary ran out, even if the sap exudate has not been completely used up. Capillary action of sap by itself did not generate an electrospray from the glass capillary tip when no electrospray solution was preloaded inside the capillary. This suggested that mixing between sap entering the capillary tip through the microloader and the preloaded electrospray solution was necessary for analysis by direct ESI.

Additionally, the ion signal duration was dependent on the chemical composition of the electrospray solution. Acidified 1:1 water:methanol yielded significantly shorter signal durations than an equal volume of a 1:1:1 mixture of water:methanol:acetonitrile (other experimental conditions, such as applied voltage and capillary tip diameter, were not changed during comparisons) (Figure S2). Upon inspection of the glass capillary tip by bright-field microscopy after the ion signal dropped to zero, a mass of probably undissolved solutes appeared to have clogged the capillary tip, while a volume of water−methanol solution was still present inside the capillary (Figure S2b). The capillary tips were not clogged when 1:1:1 mixture of water:methanol:acetonitrile was used. This may be due to the relatively poor solubility of phenolic compounds from the sample in water/methanol solvents, such as flavones and their derivatives that dominated the spectra from whole sap. By reducing the percentage of water in the electrospray solution and adding acetonitrile, the solubility of whole sap may have been enhanced, and thus the capillary tip remained unclogged during the analysis.

Direct ESI-MS of Whole Sap from Infected and Uninfected Plants. To investigate the effects of infection on the transport of material through the plant's vasculature, whole sap from infected (n = 10) and uninfected (n = 7) soybean plants was analyzed by direct ESI-MS. Principal component analysis (PCA) was used to evaluate the differences between spectra from both types of sap (Figure 4a). The PCA 2D scores plot indicated good separation between the two sample types for the first two principal components, PC1 and PC2, where PC1 captured 62.2% of the model prediction and PC2 captured 15.0% (Figure 4a).

To identify the compounds that were differentially transported by sap in the two plant groups, spectral features were compared using t tests, and the results are illustrated in a volcano plot (Figure 4b). Fold change (FC), which is defined here as the ratio of metabolite intensities in the two sample types, of FC $\geq$ 2 and FC $\leq$ 0.5, and p-values of $p \leq 0.05$ were used to identify metabolites that were significantly up- and downregulated in sap from the two plant groups; 61 and 15 metabolite ions were significantly more and less abundant, respectively, in mass spectra from sap of infected plants (Figure 4b).

As the fixation of atmospheric nitrogen is a critical component of the symbiosis, we explored the transport and regulation of nitrogen-containing compounds in the sap of

https://dx.doi.org/10.1021/acs.analchem.0c00939
Anal. Chem. 2020, 92, 7299−7306

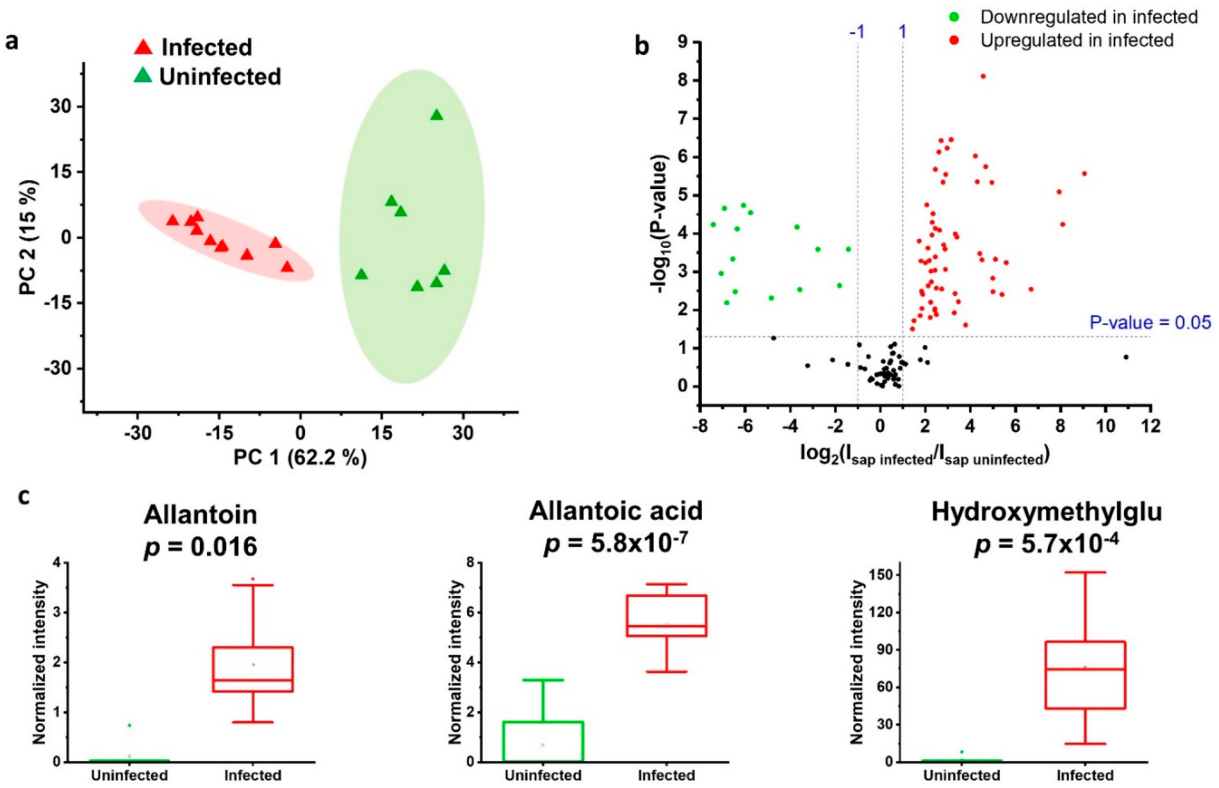

Figure 4. Multivariate statistical analysis of whole sap from infected and uninfected soybean plants. (a) PCA 2D scores plot of spectra from whole sap of infected (n = 10) and uninfected (n = 7) plants. (b) Volcano plot comparing major differences between species detected in whole sap from each group. (c) Relative abundances for three nitrogen-containing metabolites. Hydroxymethylglu: hydroxymethylglutamate.

infected plants. Ions derived from two ureides, [allantoin + Na]$^+$ (m/z 181.038) and [allantoic acid + K]$^+$ (m/z 215.011), five protein amino acids, [asparagine + H]$^+$ (m/z 133.056), [glutamic acid − H]$^-$ (m/z 146.041), [glutamine + H]$^+$ (m/z 147.077) and [lysine + K]$^+$ (m/z 185.065), and two nonprotein amino acids, [hydroxymethylglutamic acid + H]$^+$ (m/z 178.071), and [methyleneglutamic acid + H]$^+$ (m/z 160.060), were detected in whole sap by direct ESI MS/MS (Table S1). The two ureides have been shown to play a major role in nitrogen transport from the sites of nitrogen fixation to the upper parts of soybean plants.[8,9,44] In addition, amino acids, in particular asparagine and glutamine, are used for nitrogen transport through the xylem and phloem in many plants.[45,46] Glutamic acid is a central molecule in amino acid metabolism in plants, and the two nitrogen-transport amino acids, arginine and proline, are both synthesized from glutamic acid.[47] Of these nitrogen-containing metabolites, the ureides, lysine, aspartic acid, and the nonprotein amino acids were significantly more abundant in whole sap from infected plants, whereas tryptophan was downregulated (Figure 4c and Table S2). These results suggest that nitrogen transport in legumes is regulated differently, depending on the source of nitrogen supply. Although whole sap analysis does not provide information on the sources of these differences in the stem, it shows that the chemical composition of the shoot is affected by root infection.

Additionally, we observed a significant upregulation of disaccharide in sap from infected plants (Table S2). As the plant hosts its microsymbionts, it needs to provide them with energy molecules in exchange for the fixed nitrogen. Disaccharides are photoassimilates that are provided by the host and transported to the respiring bacteroids in the root nodules. Thus, the higher abundance of disaccharide in sap from infected plants provides evidence for the interdependence of the two species during the symbiosis.

Postanalysis, the plants were placed back inside the growth chamber and visual signs of growth were monitored for 14 days. The plants continued to show normal signs of growth indicated by height increase and new leaf development. Shoot development continued to take place laterally just below the cut surface.

Capillary Microsampling ESI-MS of Sap from the Xylem and Single Parenchymal Cells. Different parts of the stem, such as the pith and the vascular bundles, composed of the xylem and phloem, have different chemical compositions reflecting their biological functions. The xylem is known to provide a conduit for transporting nutrients and water from the roots to upper parts of the plant. The phloem creates a transport channel for photoassimilates from the sites of photosynthesis to other parts of the plant. The pith is composed of parenchymal cells that store and transport metabolites. To gain additional insight into the observed spectral differences between whole sap from infected and uninfected soybean plants, we analyzed and compared sap from the xylem and parenchymal cells by capillary microsampling ESI-MS (Figure 2). Due to their morphology, it was difficult to confidently identify phloem tubes without additional sample processing, e.g., staining, and to analyze their content in vivo by capillary microsampling ESI-MS.

Unlike in direct ESI-MS of the whole sap, where spatial information was not provided, capillary microsampling enabled local analysis on the micrometer scale, thus making it possible to unveil the spatial distribution of metabolites. However, the sap layer that forms on the surface due to transverse cutting

https://dx.doi.org/10.1021/acs.analchem.0c00939
Anal. Chem. 2020, 92, 7299−7306

can lead to cross-contamination between different parts of the stem, thus potentially altering the native spatial distribution of metabolites. This sap layer may inadvertently contaminate the capillary tip during sampling. Thus, to determine if the top sap layer contaminated the content of the capillary during sampling, a capillary tip preloaded with electrospray solution was lowered until it made contact with a freshly cut surface (no negative pressure was applied), and the content of the capillary was analyzed by ESI-MS. Indeed, the produced spectrum (positive ion mode) contained peaks that corresponded to compounds endogenous to the plant (Figure S3a). To mitigate this issue, a stem was cut, and the surface was left to air-dry for ∼1 min to minimize the top sap layer that covers the cut surface. Then a capillary tip preloaded with electrospray solution was lowered until it made contact with the dry surface, and the content was analyzed. The resulting spectrum did not contain peaks that corresponded to plant related ions (Figure S3b).

To sample sap from the xylem and content from single parenchymal cells in the pith separately, the capillary tip was immersed into either part after the surface was left to air-dry (∼1 min). Longer drying times caused the xylem to collapse and parenchymal cells to become flaccid. After negative pressure was applied, sample was collected from the xylem and single parenchymal cells and analyzed by ESI-MS. The produced spectra contained several common peaks (Figure 5 and Table S1). Many of these corresponded to primary metabolites such as sugars and amino acids. The presence of disaccharides in the xylem sap raises the possibility of cross-contamination due to transverse cutting of the stem, as transport of sugars is mostly associated with the phloem. There are, however, reports in the literature indicating the presence of disaccharides and hexoses in the xylem sap.[48] Importantly, many of the peaks present in the whole sap spectra were absent in the spectra from xylem sap. This observation indicates the absence of cross-contamination of the xylem sap by the whole sap.

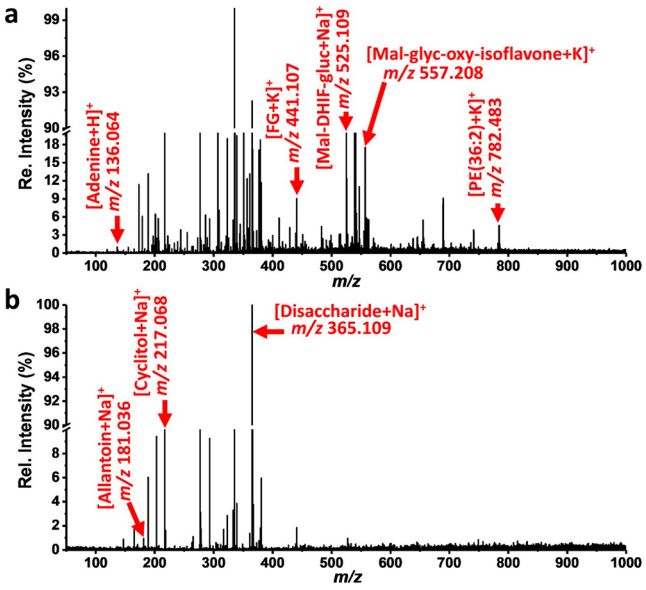

Figure 5. Capillary microsampling ESI-MS of xylem sap and parenchymal cells. Representative positive ion mode mass spectra from (a) a single parenchymal cell in the pith and (b) xylem sap of a soybean plant 21 days postinoculation with *B. japonicum*. FG: flavanone glucoside; Mal-DHIF-gluc: malonyldihydroxyisoflavone glucoside; Mal-glyc-oxy-isoflavone: malonylglycosyloxyisoflavone.

In addition, peaks corresponding to ions unique to each part of the stem were observed (Table S1). For example, several lipid classes, mainly phosphatidic acids (PAs) and phosphatidylglycerols (PGs), were not detected in the xylem. Such glycerolipids are known to be major constituents of the plasma membrane in plant cells.[49] Additionally, the two ureides, allantoin and allantoic acid, were significantly upregulated in xylem sap and parenchymal cells of infected plants. This is consistent with the notion that ureides are used for upward nitrogen transport in the sap of infected soybean plants. The presence of ureides in the neighboring parenchymal cells could be due to their transport from the xylem into these cells, where they can be metabolized into other compounds.

The presence of unique m/z peaks exclusively in mass spectra obtained from different parts of the stem, i.e., the xylem and parenchymal cells (see Table S1), minimizes the chances of potential cross-contamination. As it is possible for some compounds that originate from specific locations to have spread and dried over the surfaces of other parts, the apparent differences in the mass spectra of parenchymal cells (see Figure 5a), xylem sap (see Figure 5b), and whole sap (see Figure 3) indicate the absence of cross-contamination between the different parts of the stem.

To further understand differences between the abundances of compounds in the xylem of infected and uninfected plants, xylem sap from the two plant groups was analyzed by capillary microsampling ESI-MS. The two groups exhibited several differences in levels of N-containing compounds. Similar to what was observed in whole sap analysis, xylem sap from the infected plants exhibited higher levels of allantoin, allantoic acid, hydroxymethylglutamic acid, and methyleneglutamic acid. Counterintuitive results, revealed only by capillary microsampling ESI-MS, indicated significantly higher abundances for two nitrogen-containing metabolites, $[\text{methylglutamine} - H_2O + H]^+$ (m/z 143.080) and $[\text{valine} + K]^+$ (m/z 156.047), in the xylem sap of uninfected plants (see Figure S4). Infected plants assimilate nitrogen in the root nodules through biological nitrogen fixation by the bacteroids. On the other hand, uninfected plants absorb nitrogen-containing ions from minerals, such as nitrate, through their roots. Differences between levels of specific nitrogen-containing metabolites in the sap of infected and uninfected plants suggest that the biosynthesis of compounds for nitrogen transport is regulated differently depending on the source of nitrogen uptake by the plant.

The ability to detect certain ions by microsampling only may have been due to the lower complexity of the sample compared to direct ESI-MS of the sap, where whole sap was analyzed. As whole sap is a complex mixture of compounds that originate from different parts of the stem, ionization processes for certain chemical species, especially those that are present in low concentrations, can be more prone to ion suppression effects that manifests in their masking.[50] In microsampling, however, the sampling of specific parts of the stem reduces the complexity of the mixture resulting in reduced suppression of native low concentration compounds and less dilution of the related signal.

In addition to nitrogen-containing compounds, differences in the abundances for other metabolites in the xylem of infected and uninfected plants were explored. A total of 19 and 6 metabolite ions exhibited higher and lower intensities,

https://dx.doi.org/10.1021/acs.analchem.0c00939
Anal. Chem. 2020, 92, 7299−7306

respectively, in mass spectra from xylem sap of infected plants. Aliphatic organic acids, such as [hydroxybutanedioic acid − H − H_2O]$^-$ (m/z = 115.003), [propanedioic acid − H]$^-$ (m/z = 103.003), and [hydroxypropanetricarboxylic acid − H − H_2O]$^-$ (m/z = 173.008), and aromatic organic acids, such as [phenyllactic acid − H]$^-$ (m/z = 165.056), constituted a large proportion of the upregulated metabolites in the xylem sap of infected plants. Table S3 lists assigned up- and downregulated metabolite ions in the xylem sap of infected plants.

Parenchymal cells of infected and uninfected plants were also analyzed by capillary microsampling, and their metabolic compositions were compared. Cells from the infected plants exhibited higher and lower abundances for 29 and 7 metabolite ions, respectively. Sugars, such as mono- and disaccharides, their derivatives, such as hexose phosphate, and sugar-linked compounds, such as [hydroxymethylflavanone hexoside + K]$^+$ (m/z = 439.119), were upregulated in the parenchymal cells of infected plants. Additionally, nitrogen-containing compounds that were upregulated in these cells included [ornithine + K]$^+$ (m/z = 171.051), [oxoproline + H]$^+$ (m/z = 130.049), and [lysine + K]$^+$ (m/z = 185.065). The fold change values for these compounds and others in the parenchymal cells of infected plants relative to the uninfected ones are shown in Table S4.

CONCLUSIONS

Direct ESI-MS enabled fast and simple in vivo analysis of sap from plants in their native environment. This enabled the analysis of living plants grown under different conditions of nitrogen supply and, thus, provided insight into their effects on the transport of nitrogen and other metabolites through the plant's vasculature. When combined with capillary microsampling, spatial information was unveiled, which provided insight into the metabolites transported by the xylem and the composition of parenchymal cells.

Recent results on plant transport systems have shown that they perform complex trafficking of signaling molecules and developmental regulators, enabling plants to adapt to their environment.[51−53] With the continuous improvement in the sensitivity of mass spectrometers, and with a short analysis time that spans less than 1 min, in vivo analysis by direct ESI-MS holds promise for real-time monitoring of fast physiological responses in plants to external stimuli, thus potentially elucidating mechanisms of long-distance signal transduction.

ASSOCIATED CONTENT

Supporting Information

The Supporting Information is available free of charge at https://pubs.acs.org/doi/10.1021/acs.analchem.0c00939.

Images of soybean plants analyzed by direct and capillary microsampling, effect of spray solution composition on ion signal duration, contamination of capillary tip by exudate, downregulation of two nitrogen-containing metabolites in xylem sap, metabolite assignments from whole sap, xylem sap, and parenchymal cells, relative abundances of metabolites differentially regulated in whole sap, xylem sap, and in parenchymal cells (PDF)

AUTHOR INFORMATION

Corresponding Author

Akos Vertes − *Department of Chemistry, George Washington University, Washington, DC 20052, United States;* orcid.org/0000-0001-5186-5352; Phone: +1 (202) 994-2717; Email: vertes@gwu.edu; Fax: +1 (202) 994-5873

Authors

Laith Z. Samarah − *Department of Chemistry, George Washington University, Washington, DC 20052, United States*

Tina H. Tran − *Department of Chemistry, George Washington University, Washington, DC 20052, United States*

Gary Stacey − *Divisions of Plant Sciences and Biochemistry, C. S. Bond Life Sciences Center, University of Missouri, Columbia, Missouri 65211, United States*

Complete contact information is available at: https://pubs.acs.org/10.1021/acs.analchem.0c00939

Author Contributions

A.V. and G.S. conceived the research. A.V. and L.Z.S. designed the experimental setup for direct ESI-MS. L.Z.S. and T.H.T. performed the experiments. A.V., L.Z.S., and T.H.T. analyzed the data. L.Z.S. wrote the manuscript with input from A.V. and G.S.

Notes

The authors declare no competing financial interest.

ACKNOWLEDGMENTS

This work is supported by the National Science Foundation Plant Genome Program under grant no. IoS-1734145 awarded to G.S.

REFERENCES

(1) So, P. K.; Hu, B.; Yao, Z. P. *Mol. BioSyst.* **2013**, *9*, 915−929.

(2) Fatou, B.; Saudemont, P.; Leblanc, E.; Vinatier, D.; Mesdag, V.; Wisztorski, M.; Focsa, C.; Salzet, M.; Ziskind, M.; Fournier, I. *Sci. Rep.* **2016**, *6*, 25919.

(3) Schafer, K. C.; Denes, J.; Albrecht, K.; Szaniszlo, T.; Balog, J.; Skoumal, R.; Katona, M.; Toth, M.; Balogh, L.; Takats, Z. *Angew. Chem., Int. Ed.* **2009**, *48*, 8240−8242.

(4) Zhang, J. L.; Rector, J.; Lin, J. Q.; Young, J. H.; Sans, M.; Katta, N.; Giese, N.; Yu, W. D.; Nagi, C.; Suliburk, J.; Liu, J. S.; Bensussan, A.; DeHoog, R. J.; Garza, K. Y.; Ludolph, B.; Sorace, A. G.; Syed, A.; Zahedivash, A.; Milner, T. E.; Eberlin, L. S. Nondestructive tissue analysis for ex vivo and in vivo cancer diagnosis using a handheld mass spectrometry system. *Sci. Transl. Med.* **2017**, *9*, eaan3968

(5) Jensen, K. H.; Berg-Sorensen, K.; Bruus, H.; Holbrook, N. M.; Liesche, J.; Schulz, A.; Zwieniecki, M. A.; Bohr, T. Sap flow and sugar transport in plants. *Rev. Mod. Phys.*, **2016**, *88*, DOI: 10.1103/RevModPhys.88.035007

(6) Karve, A. A.; Alexoff, D.; Kim, D.; Schueller, M. J.; Ferrieri, R. A.; Babst, B. A. In vivo quantitative imaging of photoassimilate transport dynamics and allocation in large plants using a commercial positron emission tomography (PET) scanner. *BMC Plant Biol.* **2015**, *15*, DOI: 10.1186/s12870-015-0658-3

(7) Cohn, J.; Day, R. B.; Stacey, G. *Trends Plant Sci.* **1998**, *3*, 105−110.

(8) Masuda, R.; Sugimoto, T.; Shiraishi, N.; Ohyama, T.; Oji, Y. *Soil Sci. Plant Nutr.* **2003**, *49*, 185−190.

(9) McClure, P. R.; Israel, D. W. *Plant Physiol.* **1979**, *64*, 411−416.

(10) Li, B. B.; Feng, Z. G.; Xie, M.; Sun, M. Z.; Zhao, Y. X.; Liang, L. Y.; Liu, G. J.; Zhang, J. H.; Jia, W. S. *J. Exp. Bot.* **2011**, *62*, 1731−1741.

(11) Netting, A. G.; Theobald, J. C.; Dodd, I. C. Xylem sap collection and extraction methodologies to determine in vivo concentrations of ABA and its bound forms by gas chromatography-mass spectrometry (GC-MS). *Plant Methods* **2012**, *8*, 11

(12) Li, L.; Zhang, Q.; Huang, D. F. *Sensors* **2014**, *14*, 20078−20111.

(13) Hubeau, M.; Steppe, K. *Trends Plant Sci.* **2015**, *20*, 676−685.

(14) Partelova, D.; Uhrovcik, J.; Lesny, J.; Hornik, M.; Rajec, P.; Kovac, P.; Hostin, S. *Chemical Papers* **2014**, *68*, 1463−1473.
(15) Kiser, M. R.; Reid, C. D.; Crowell, A. S.; Phillips, R. P.; Howell, C. R. *HFSP J.* **2008**, *2*, 189−204.
(16) Kawachi, N.; Kikuchi, K.; Suzui, N.; Ishii, S.; Fujimaki, S.; Ishioka, N. S.; Watabe, H. *IEEE Trans. Nucl. Sci.* **2011**, *58*, 395−399.
(17) Jahnke, S.; Menzel, M. I.; van Dusschoten, D.; Roeb, G. W.; Buhler, J.; Minwuyelet, S.; Blumler, P.; Temperton, V. M.; Hombach, T.; Streun, M.; Beer, S.; Khodaverdi, M.; Ziemons, K.; Coenen, H. H.; Schurr, U. *Plant J.* **2009**, *59*, 634−644.
(18) Kaspar, S.; Peukert, M.; Svatos, A.; Matros, A.; Mock, H. P. *Proteomics* **2011**, *11*, 1840−1850.
(19) Bjarnholt, N.; Li, B.; D'Alvise, J.; Janfelt, C. *Nat. Prod. Rep.* **2014**, *31*, 818−837.
(20) Tanaka, K.; Waki, H.; Ido, Y.; Akita, S.; Yoshida, Y.; Yoshida, T.; Matsuo, T. *Rapid Commun. Mass Spectrom.* **1988**, *2*, 151−153.
(21) Velickovic, D.; Agtuca, B. J.; Stopka, S. A.; Vertes, A.; Koppenaal, D. W.; Pasa-Tolic, L.; Stacey, G.; Anderton, C. R. *ISME J.* **2018**, *12*, 2335−2338.
(22) Walker, B. N.; Stolee, J. A.; Pickel, D. L.; Retterer, S. T.; Vertes, A. *J. Phys. Chem. C* **2010**, *114*, 4835−4840.
(23) Takats, Z.; Wiseman, J. M.; Gologan, B.; Cooks, R. G. *Science* **2004**, *306*, 471−473.
(24) Nemes, P.; Vertes, A. *Anal. Chem.* **2007**, *79*, 8098−8106.
(25) Nemes, P.; Vertes, A. *TrAC, Trends Anal. Chem.* **2012**, *34*, 22−34.
(26) Cody, R. B.; Laramee, J. A.; Durst, H. D. *Anal. Chem.* **2005**, *77*, 2297−2302.
(27) Liu, J. J.; Wang, H.; Cooks, R. G.; Ouyang, Z. *Anal. Chem.* **2011**, *83*, 7608−7613.
(28) Pereira, I.; Rodrigues, S. R. M.; de Carvalho, T. C.; Carvalho, V. V.; Lobon, G. S.; Bassane, J. F. P.; Domingos, E.; Romao, W.; Augusti, R.; Vaz, B. G. *Anal. Methods* **2016**, *8*, 6023−6029.
(29) Hu, B.; Wang, L.; Ye, W. C.; Yao, Z. P. *Sci. Rep.* **2013**, *3*, 2104.
(30) Shrestha, B.; Vertes, A. *Anal. Chem.* **2009**, *81*, 8265−8271.
(31) Samarah, L. Z.; Khattar, R.; Tran, T. H.; Stopka, S. A.; Brantner, C. A.; Parlanti, P.; Veličković, D.; Shaw, J. B.; Agtuca, B. J.; Stacey, G.; Paša-Tolić, L.; Tolić, N.; Anderton, C. R.; Vertes, A. Single-Cell Metabolic Profiling: Metabolite Formulas from Isotopic Fine Structures in Heterogeneous Plant Cell Populations. *Anal. Chem.* **2020**, *92*, in press. DOI: 10.1021/acs.analchem.0c00936
(32) Kompauer, M.; Heiles, S.; Spengler, B. *Nat. Methods* **2017**, *14*, 90−96.
(33) Bergman, H. M.; Lanekoff, I. *Analyst* **2017**, *142*, 3639−3647.
(34) Mizuno, H.; Tsuyama, N.; Date, S.; Harada, T.; Masujima, T. *Anal. Sci.* **2008**, *24*, 1525−1527.
(35) Zhang, L. W.; Foreman, D. P.; Grant, P. A.; Shrestha, B.; Moody, S. A.; Villiers, F.; Kwak, J. M.; Vertes, A. *Analyst* **2014**, *139*, 5079−5085.
(36) Lee, J. K.; Jansson, E. T.; Nam, H. G.; Zare, R. N. *Anal. Chem.* **2016**, *88*, 5453−5461.
(37) Pan, N.; Rao, W.; Kothapalli, N. R.; Liu, R. M.; Burgett, A. W. G.; Yang, Z. B. *Anal. Chem.* **2014**, *86*, 9376−9380.
(38) Tomos, A. D.; Sharrock, R. A. *J. Exp. Bot.* **2001**, *52*, 623−630.
(39) Stopka, S. A.; Agtuca, B. J.; Koppenaal, D. W.; Pasa-Tolic, L.; Stacey, G.; Vertes, A.; Anderton, C. R. *Plant J.* **2017**, *91*, 340−354.
(40) Stopka, S. A.; Samarah, Z. L.; Shaw, J.; Liyu, A.; Velickovic, D.; Agtuca, B.; Kukolj, C.; Koppenaal, D.; Stacey, G.; Pasa-Tolic, L.; Anderton, C.; Vertes, A. *Anal. Chem.* **2019**, *91*, 5028−5035.
(41) Cole, M. A.; Elkan, G. H. *Antimicrob. Agents Chemother.* **1973**, *4*, 248−253.
(42) Broughton, W. J.; Dilworth, M. J. *Biochem. J.* **1971**, *125*, 1075−1080.
(43) Zhang, L. W.; Vertes, A. *Anal. Chem.* **2015**, *87*, 10397−10405.
(44) Collier, R.; Tegeder, M. *Plant J.* **2012**, *72*, 355−367.
(45) Tegeder, M.; Masclaux-Daubresse, C. *New Phytol.* **2018**, *217*, 35−53.
(46) Tegeder, M. *J. Exp. Bot.* **2014**, *65*, 1865−1878.
(47) Forde, B. G.; Lea, P. J. *J. Exp. Bot.* **2007**, *58*, 2339−2358.
(48) Bonhomme, M.; Peuch, M.; Ameglio, T.; Rageau, R.; Guilliot, A.; Decourteix, M.; Alves, G.; Sakr, S.; Lacointe, A. *Tree Physiol.* **2010**, *30*, 89−102.
(49) Cacas, J. L.; Bure, C.; Grosjean, K.; Gerbeau-Pissot, P.; Lherminier, J.; Rombouts, Y.; Maes, E.; Bossard, C.; Gronnier, J.; Furt, F.; Fouillen, L.; Germain, V.; Bayer, E.; Cluzet, S.; Robert, F.; Schmitter, J. M.; Deleu, M.; Lins, L.; Simon-Plas, F.; Mongrand, S. *Plant Physiol.* **2016**, *170*, 367−384.
(50) Zhang, L. W.; Khattar, N.; Kemenes, I.; Kemenes, G.; Zrinyi, Z.; Pirger, Z.; Vertes, A. *Sci. Rep.* **2018**, *8*, 12227.
(51) Lopez-Salmeron, V.; Cho, H.; Tonn, N.; Greb, T. *Curr. Biol.* **2019**, *29*, R173−R181.
(52) Notaguchi, M.; Okamoto, S. *Front. Plant Sci.* **2015**, *6*, 161.
(53) Oh, E.; Seo, P. J.; Kim, J. *Trends Plant Sci.* **2018**, *23*, 337−351.

https://dx.doi.org/10.1021/acs.analchem.0c00939
Anal. Chem. 2020, 92, 7299−7306

Supporting Information

In vivo Chemical Analysis of Plant Sap from the Xylem and Single Parenchymal Cells by Capillary Microsampling Electrospray Ionization Mass Spectrometry

Laith Z. Samarah,† Tina H. Tran,† Gary Stacey‡ and Akos Vertes,†*

†Department of Chemistry, George Washington University, Washington, DC 20052

‡ Divisions of Plant Sciences and Biochemistry, C. S. Bond Life Sciences Center, University of Missouri, Columbia, MO 65211

*Corresponding Author
E-mail: vertes@gwu.edu. Phone: +1 (202) 994-2717. Fax: +1 (202) 994-5873.

Table of Contents

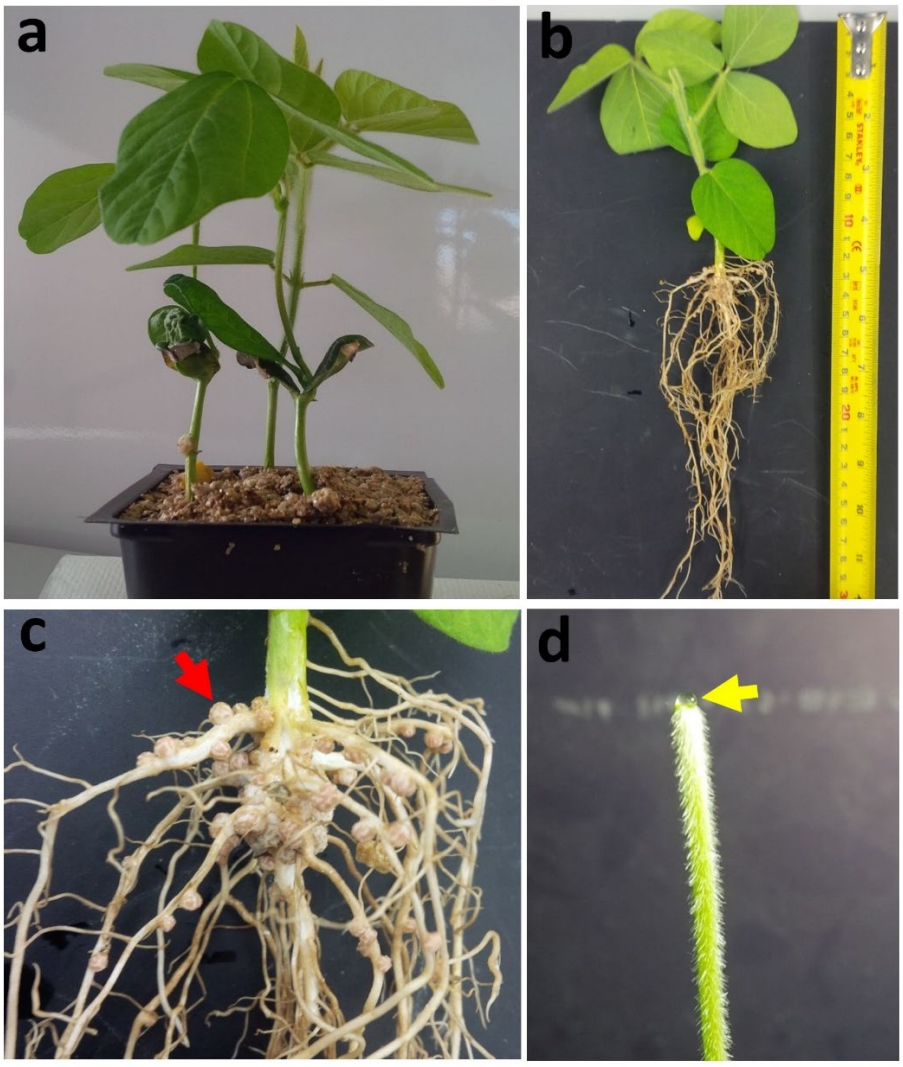

Figure S1. Photographic images of soybean plants analyzed by direct and capillary microsampling ESI-MS. (a) Soybean plant 21 days after inoculation by *wt B. japonicum*. (b) An infected soybean plant taken out of the soil. (c) Root nodule (red arrow), the organ where atmospheric nitrogen fixation takes place, 21 days post inoculation. (d) Sap exudate (yellow arrow) formed spontaneously after cutting the stem ~5 mm below the shoot apical meristem.

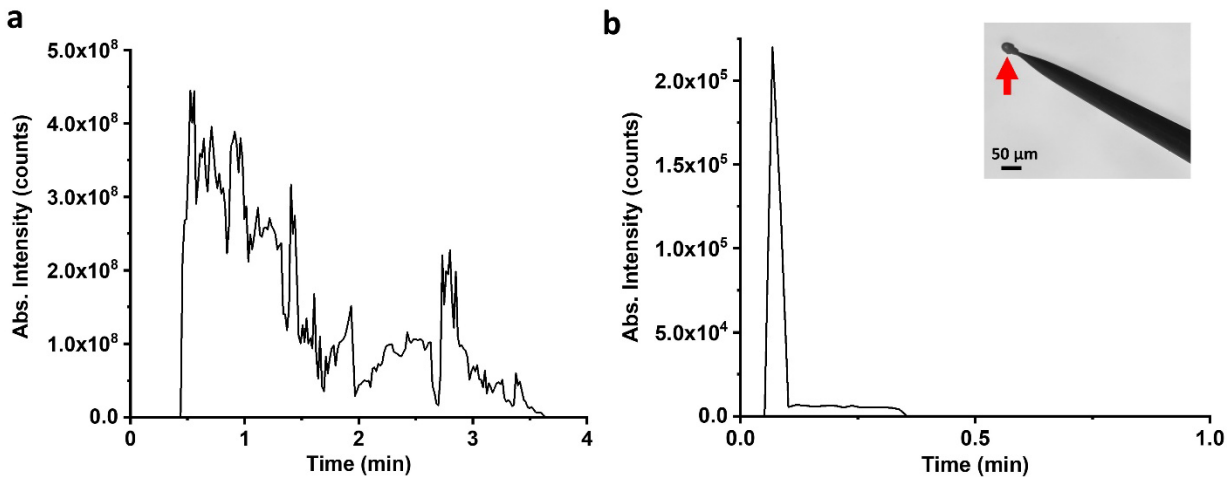

Figure S2. Effect of spray solution composition on ion signal duration in direct ESI-MS. Typical ion chromatograms for disaccharide (*m/z* 381.084) obtained by direct ESI-MS of whole sap from a soybean plant using (a) 1:1:1 acidified water:methanol:acetonitrile and (b) 1:1 acidified water:methanol as electrospray solutions. The microscope image in the inset shows a glass capillary tip preloaded with 1:1 acidified water:methanol and clogged by a precipitate (red arrow) from whole sap. The image was taken after the ion signal dropped to zero.

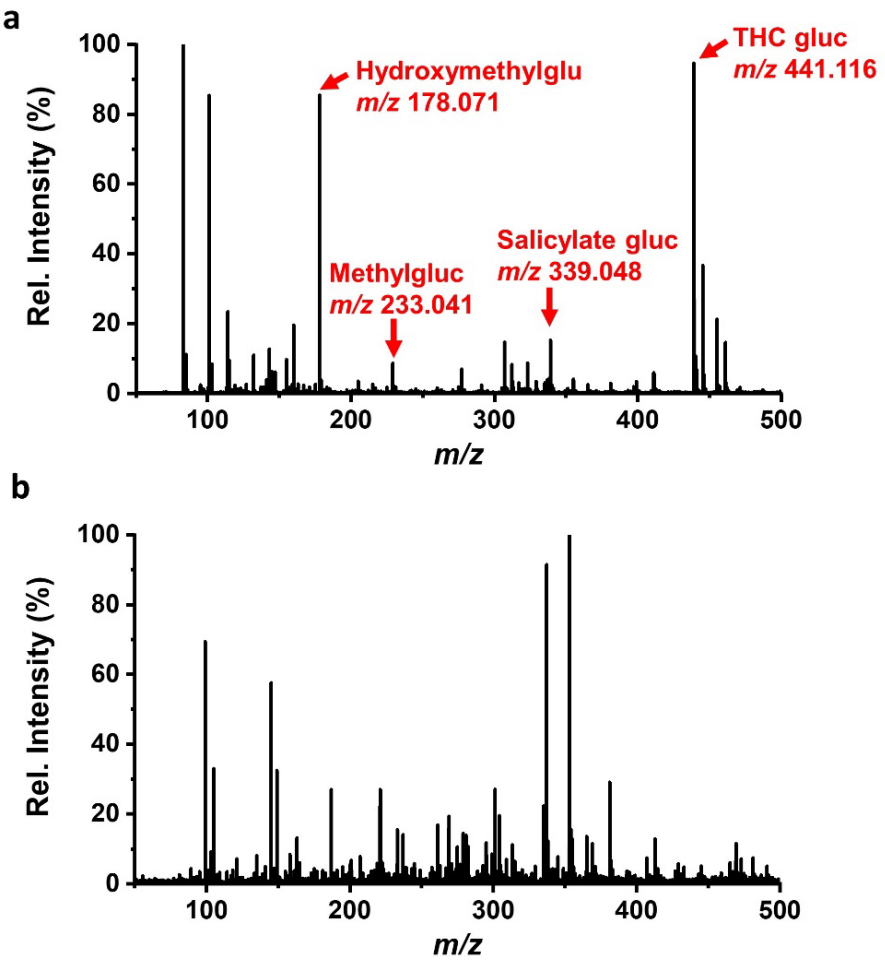

Figure S3. Contamination of capillary tip by exudate on freshly cut stem surface. (a) Positive-ion mode mass spectrum produced by touching the wet surface of a freshly cut stem with the capillary tip (no negative pressure applied). Ions corresponding to endogenous compounds from the plant can be seen in the spectrum (labeled in red). (b) After waiting for the surface to air-dry (~1 min), analysis of the capillary content after touching the surface with the capillary tip produced exclusively electrospray background peaks (positive ion mode). Methylgluc: methylglucoside; Salicylate gluc: salicylate glucoside; THC gluc: trihydroxychalcone glucoside; Hydroxymethylglu: hydroxymethylglutamate.

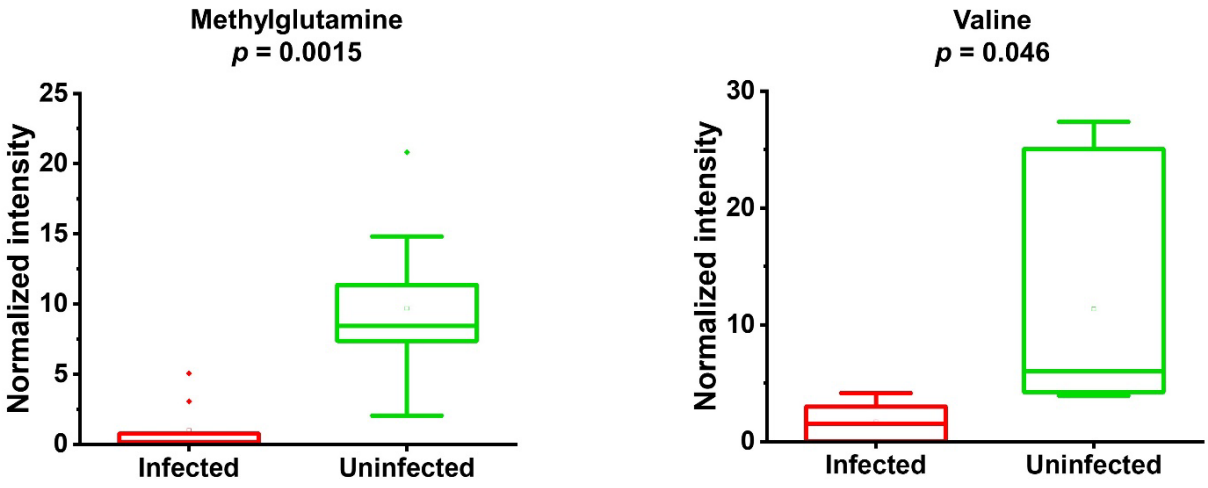

Figure S4. Downregulation of two nitrogen-containing metabolites in xylem sap of infected soybean plants revealed exclusively by capillary microsampling ESI-MS.

Table S1. Metabolite assignments from whole sap, xylem sap, and parenchymal cells of the pith.

Compound	Ion type	Measured mass	Calculated mass	Δm (ppm)	MSI level[a]	Whole sap	Xylem	Pith cells
Adenine	$[M+H-2H_2O]^+$	100.039	100.042	-30	2	✓	✓	✓
Glyceraldehyde	$[M+Na]^+$	113.009	113.021	-107	3	✓	×	✓
Cyanoalanine	$[M+H]^+$	115.039	115.051	-104	3	✓	×	✓
Fumarate	$[M+H]^+$	117.021	117.019	17	3	✓	×	✓
Succinate	$[M+H]^+$	119.049	119.060	-92	3	✓	✓	✓
Hydroxymalonate	$[M+H]^+$	121.017	121.014	25	3	✓	✓	✓
Salicylaldehyde	$[M+H]^+$	123.042	123.044	-16	2	✓	✓	✓
Hydroxybutanoate	$[M+Na]^+$	127.029	127.037	-63	3	✓	✓	✓
Oxoproline	$[M+H]^+$	130.048	130.050	-15	2	✓	✓	✓
Asparagine	$[M+H]^+$	133.064	133.061	23	2	✓	✓	✓
Aspartate	$[M+H]^+$	134.035	134.045	-75	2	✓	✓	✓
Malate	$[M+H]^+$	135.036	135.029	52	2	✓	✓	✓
Adenine	$[M+H]^+$	136.064	136.062	15	2	✓	✓	✓
Methylbutanoate	$[M+K]^+$	141.037	141.032	35	3	✓	✓	✓
Threonine	$[M+Na]^+$	142.044	142.048	-28	3	✓	✓	✓
Methylglutamine	$[M+H-H_2O]^+$	143.081	143.082	-7	3	×	✓	×
Cysteine	$[M+Na]^+$	144.021	144.009	83	3	✓	✓	✓
Glutamic acid	$[M-H]^-$	146.041	146.046	-34	2	✓	✓	✓
Coumarin	$[M+H]^+$	147.041	147.045	-27	2	✓	×	✓
Glutamine	$[M+H]^+$	147.077	147.076	7	2	×	✓	✓
Valine	$[M+K]^+$	156.047	156.043	26	2	×	✓	×
Hydroxyisovalerate	$[M+K]^+$	157.024	157.027	-19	3	✓	×	✓
Allantoin	$[M+H]^+$	159.049	159.052	-19	1	✓	✓	✓
Methyleneglutamate	$[M+H]^+$	160.060	160.060	0	2	✓	✓	✓
Salicylate	$[M+Na]^+$	161.030	161.022	50	2	✓	✓	✓
Ornithine	$[M+K]^+$	171.049	171.054	-29	3	✓	×	✓
Pentose	$[M+Na]^+$	173.027	173.042	-87	3	✓	✓	✓
Arginine	$[M+H]^+$	175.135	175.120	86	2	✓	✓	✓
Hydroxymethylglutamate	$[M+H]^+$	178.071	178.071	0	2	✓	✓	✓
Allantoin	$[M+Na]^+$	181.038	181.034	22	1	✓	✓	✓
Methylglutamate	$[M+Na]^+$	184.046	184.058	-65	2	✓	✓	✓
Glutamine	$[M+K]^+$	185.031	185.033	-11	2	✓	✓	✓
Lysine	$[M+K]^+$	185.065	185.069	-22	2	✓	✓	✓
Dihydrocoumarin	$[M+K]^+$	187.017	187.016	5	3	✓	×	✓
Dihydroxybenzoate	$[M+K]^+$	193.001	192.991	52	2	✓	✓	✓
Shikimate	$[M+Na]^+$	197.035	197.042	-36	3	✓	✓	✓
Hydroxymethylglutarate	$[M+K]^+$	201.009	201.016	-35	3	✓	×	✓
Hexose	$[M+Na]^+$	203.073	203.053	98	2	✓	✓	✓

Homocitrate	$[M+H]^+$	207.046	207.050	-19	2	✓	×	✓
Acetylglutamate	$[M+Na]^+$	212.038	212.053	-71	3	✓	×	✓
Allantoic acid	$[M+K]^+$	215.011	215.018	-33	2	✓	✓	✓
Cyclitol	$[M+Na]^+$	217.066	217.070	-18	2	✓	✓	✓
Hexose	$[M+K]^+$	219.024	219.027	-14	2	✓	✓	✓
Mevalonate phosphate	$[M+H]^+$	229.055	229.048	31	3	✓	×	✓
Methylglucoside	$[M+K]^+$	233.041	233.043	-9	3	✓	×	✓
Sinapate	$[M+Na]^+$	247.062	247.058	16	3	✓	×	✓
Hydroxytryptophan	$[M+K]^+$	259.052	259.068	-62	3	✓	✓	✓
Acetylhexosamine	$[M+K]^+$	260.060	260.054	23	2	✓	×	✓
Hexose phosphate	$[M+H]^+$	261.057	261.038	73	3	✓	×	✓
Phosphotyrosine	$[M+H]^+$	262.058	262.048	38	3	✓	×	✓
Trihydroxyflavone	$[M+H]^+$	271.045	271.060	-55	3	✓	✓	✓
Methoxyisoflavone	$[M+Na]^+$	275.058	275.068	-36	3	✓	×	✓
Methoxyflavanone	$[M+Na]^+$	277.075	277.084	-32	3	✓	×	✓
Dihydroxyflavanone	$[M+Na]^+$	279.075	279.063	43	3	✓	×	✓
Hexose phosphate	$[M+Na]^+$	282.999	283.019	-71	3	✓	×	✓
tetrahydroxyisoflavanone	$[M+H]^+$	289.065	289.071	-21	3	✓	×	✓
Dihydroxymethoxyflavone	$[M+Na]^+$	307.067	307.058	29	3	✓	×	✓
Dihydroxymethoxyisoflavanone	$[M+Na]^+$	309.079	309.074	16	3	✓	×	✓
Monomethoxyflavone	$[M+H]^+$	317.070	317.066	13	3	✓	×	✓
Dimethoxyflavone	$[M+K]^+$	321.046	321.053	-22	3	✓	×	✓
Methylkaempferol	$[M+Na]^+$	323.060	323.053	22	3	✓	✓	✓
Trihydroxymethoxyisoflavanone	$[M+Na]^+$	325.064	325.070	-18	3	✓	×	✓
Apiofuranosylhexose	$[M+Na]^+$	335.086	335.095	-27	3	✓	✓	✓
Salicylate glucoside	$[M+K]^+$	339.054	339.048	18	2	✓	✓	✓
Trihydroxyflavanone	$[M+K]^+$	341.056	341.043	38	3	✓	×	✓
Rhamnosylhexose	$[M+Na]^+$	349.103	349.111	-23	3	✓	×	✓
Pentahydroxymethoxyflavone	$[M+Na]^+$	355.045	355.043	6	3	✓	×	✓
Disaccharide	$[M+Na]^+$	365.108	365.106	5	2	✓	✓	✓
Disaccharide	$[M+K]^+$	381.082	381.079	8	2	✓	✓	✓
A gibberellin	$[M+K]^+$	385.092	385.105	-34	3	✓	✓	✓
Sinapaldehyde glucoside	$[M+Na]^+$	393.121	393.116	13	2	✓	✓	✓
Hexahydroxyflavone	$[M+Na]^+$	397.089	397.090	-3	3	✓	×	✓
Methylguanosine phosphate	$[M+Na]^+$	401.077	401.071	15	3	✓	×	✓
Tuberonic acid glucoside	$[M+Na]^+$	411.154	411.163	-22	2	✓	×	✓
Trihydroxychalcone glucoside	$[M+Na]^+$	441.119	441.116	7	3	✓	×	✓
Kaempferol rhamnoside	$[M+Na]^+$	455.096	455.095	2	3	✓	✓	✓
Methylflavone glucoside	$[M+Na]^+$	469.126	469.111	32	3	✓	×	✓
Trihydroxyflavanone glucoside	$[M+Na]^+$	487.121	487.122	-2	3	✓	×	✓
Malonyldihydroxyisoflavone	$[M+Na]^+$	525.109	525.120	-21	3	✓	×	✓
Malonylglycosyloxyisoflavone	$[M+K]^+$	557.208	557.219	-20	3	✓	×	✓

PA (36:4)	$[M+K]^+$	735.483	735.436	64	2	✓	×	✓
PA (36:3)	$[M+K]^+$	737.443	737.451	-11	2	✓	×	✓
PA (36:2)	$[M+K]^+$	739.458	739.467	-12	2	✓	×	✓
PE (34:2)	$[M+K]^+$	754.469	754.478	-12	2	✓	×	✓
PE (34:1)	$[M+K]^+$	756.483	756.494	-15	2	✓	×	✓
PE (36:2)	$[M+K]^+$	782.483	782.509	-33	2	✓	×	✓
PG (34:3)	$[M-H]^-$	743.456	743.487	-42	2	✓	×	✓
PG (34:2)	$[M-H]^-$	745.536	745.502	46	2	✓	×	✓
PG (34:1)	$[M-H]^-$	747.526	747.518	11	2	✓	×	✓

Tick marks and crosses refer to detected and not detected compounds, respectively.
[a]Metabolomics Standards Initiative (MSI) levels of identification: Level 1 necessitates that 2 or more orthogonal properties of a chemical standard (here, measured mass of the compound and its tandem MS) analysed in a laboratory are compared to experimental data acquired in the same laboratory with the same analytical methods. Level 2 requires that 2 or more orthogonal properties of a compound (here, also measured mass of the compound and its tandem MS) are compared with external reported literature values. Level 3 annotation is based on comparison of the compound's measured *m/z* with the calculated value.

Table S2. Relative abundances of metabolites differentially regulated in whole sap from infected and uninfected soybean plants.

Category	Compound	MSI level	log_2(FC)[a]	*p*-value[b]
$I_{infected}/I_{uninfected}$	Adenine	2	1.85	9.16E-03
	Disaccharide	2	1.88	3.60E-04
	Hydroxylysine	3	2.06	1.78E-05
	Hydroxymethylglutarate	3	2.06	1.78E-05
	Coumarin	2	2.17	5.11E-04
	Allantoin	1	2.21	1.57E-02
	Hexose	2	2.23	6.27E-03
	Methylsalicylaldehyde	2	2.24	9.69E-04
	Sinapyl aldehyde	2	2.30	5.10E-05
	Methylglutamate	2	2.44	2.10E-06
	Dihydrocoumarin	3	2.49	2.68E-03
	Acetylhexoseamine	2	2.78	4.55E-06
	Phenyllactic acid	2	2.89	8.66E-04
	Allantoic acid	2	2.96	5.85E-07
	Ureidohomoserine	3	3.05	4.50E-02
	Sinapic acid	2	3.11	6.80E-04
	Deoxyhexose-phosphate	3	3.14	3.51E-07
	Hydroxybutanoate	2	3.28	1.18E-02
	Cystine	3	3.31	3.69E-03
	Methylglucoside	3	3.46	6.12E-03
	Oxoproline	2	4.26	4.20E-05
	Aspartic acid	2	4.41	9.60E-06
	Methyleneglutamate	2	4.51	4.87E-04
	Ornithine	3	4.56	7.71E-09
	Hydroxymethylglutamic acid	2	5.59	5.78E-04
	Lysine	2	7.94	8.19E-06
	Glycerotetrulose phosphate	3	9.06	2.71E-06
	An estradiol	2	-7.42	5.86E-05
	Inosine phosphate	3	-7.06	1.11E-03
	Tryptophan	2	-6.81	6.46E-03
	Galloylhexose	3	-6.55	4.63E-04
	Acetylneuraminic acid	3	-6.44	3.32E-03
	Glycosylasparagine	3	-6.05	1.20E-03
	Shikimate phosphate	3	-3.70	6.78E-05
	Trihydroxymethoxyflavanone	3	-2.77	2.60E-04
	Tetrahydroxymethoxyflavanone	3	-1.82	2.30E-03
	Hydroxydimethoxyflavanone	3	-1.42	2.59E-04

[a]Fold change (FC) is the ratio of the intensity of a given compound in one group to the other. The cutoff value for the fold change is 2.
[b]Threshold for the *p*-value calculated from *t*-test is 0.05.
Color code for compound names: red, compounds upregulated in whole sap from infected plants; green, downregulated compounds in whole sap of infected plants.

Table S3. Relative abundances of metabolites differentially regulated in xylem sap from infected and uninfected soybean plants.

Category	Compound	MSI level	log_2(FC)[a]	*p*-value[b]
$I_{infected}/I_{uninfected}$	Phenyllactic acid	2	1.18	4.04E-02
	Ureidohomoserine	3	1.48	3.66E-02
	Butyric acid	2	1.83	4.90E-04
	Methyleneglutamate	2	1.87	3.75E-02
	Disaccharide	2	1.96	4.06E-02
	Allantoin	1	2.02	5.06E-04
	Allantoic acid	2	2.12	9.20E-04
	Dimethylbutanedioic acid	3	2.12	1.12E-02
	Hydroxymethylglutamic acid	2	2.13	1.14E-02
	Propanedioic acid	2	2.51	6.71E-03
	Hydroxybutanoate	2	2.92	2.50E-02
	Hydroxypropane-tricarboxylic acid	2	3.60	2.05E-06
	Hydroxybutandioic acid	2	3.69	2.14E-02
	Dimethoxycinnamic acid	3	4.61	3.44E-02
	Formylsalicylic acid	3	5.56	1.40E-02
	Methylglutamine	3	-3.16	1.46E-03
	Valine	3	-2.44	4.56E-02
	Inosine phosphate	3	-1.85	3.76E-02
	Acetylneuraminic acid	2	-1.53	1.10E-03
	Propanediolhexopyranoside	3	-1.21	2.51E-02
	Shikimate phosphate	3	-1.07	4.50E-02

[a]Fold change (FC) is the ratio of the intensity of a given compound in one group to the other. The cutoff value for the fold change is 2.
[b]Threshold for the *p*-value calculated from *t*-test is 0.05.
Color code for compound names: red, compounds upregulated in xylem sap from infected plants; green, downregulated compounds in xylem sap of infected plants.

Table S4. Relative abundances of metabolites differentially regulated in parenchymal cells from infected and uninfected soybean plants.

Category	Compound	MSI level	log_2(FC)[a]	*p*-value[b]
$I_{infected}/I_{uninfected}$	Allantoin	1	1.29	9.16E-03
	Hydroxybutanedioic acid	2	1.53	2.26E-02
	Methylglutamate	2	1.75	3.61E-02
	Acetylhexosamine	2	1.94	7.59E-03
	Diethylhydroxybutanedioic acid	3	2.04	1.20E-05
	Hydroxydimethoxymethylenedioxyflavone hexoside	3	2.21	1.49E-02
	Trihydroxydimethylflavone hexoside	3	2.31	1.48E-04
	Deoxyheptulose phosphate	3	2.44	2.79E-05
	Hexose phosphate	2	2.49	2.66E-05
	Disaccharide	2	2.58	3.95E-03
	Trihydroxydimethoxyflavone hexoside	2	2.75	8.30E-04
	Aminobutanoic acid	3	2.76	5.20E-03
	Adenine	2	2.84	9.69E-05
	Hexose	2	2.97	1.60E-02
	Phenyllactic acid	2	3.66	3.20E-03
	Trimethoxyphenyl hexoside	3	3.73	1.68E-03
	Methylbutenoic acid	2	3.77	4.01E-03
	Oxoproline	2	3.84	2.99E-06
	Ornithine	3	4.08	6.65E-07
	Hydroxymethylflavanone hexoside	2	4.64	1.30E-02
	Methylbenzoic acid	3	4.99	5.85E-03
	Lysine	2	5.52	1.60E-04
	Acetylalanine	3	5.96	1.15E-04
	Hydroxyproline	2	6.12	1.08E-04
	Hydroxydimethoxyflavanone	3	-5.63	7.12E-05
	Inosine diphosphate	3	-5.35	8.11E-05
	Trihydroxyflavone	3	-4.74	1.05E-02
	Tryptophan	2	-4.00	7.10E-10
	Trihydroxytrimethoxyisoflavone glucoside	3	-3.86	1.32E-02
	Heptamethoxyflavone	3	-2.68	8.48E-04

[a]Fold change (FC) is the ratio of the intensity of a given compound in one group to the other. The cutoff value for the fold change is 2.
[b]Threshold for the *p*-value calculated from *t*-test is 0.05.
Color code for compound names: red, compounds upregulated in parenchymal from infected plants; green, downregulated compounds in parenchymal cells of infected plants.